

Crystallographic studies of olivine-related sarcopside-type solid solutions

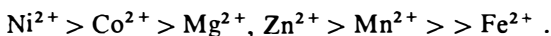
Anders G. Nord

Section of Mineralogy, Swedish Museum of Natural History,
P.O. Box 50007, S-104 05 Stockholm 50, Sweden

Received: May 9, 1983

Cation distribution / Sarcopside / Orthophosphate / Neutron diffraction

Abstract. Solid solutions of $Me_3(PO_4)_2$ in $Ni_3(PO_4)_2$, with the olivine-related sarcopside structure ($P2_1/a$), have been prepared and equilibrated at 1070 K ($Me = Mg, Mn, Fe, Co, Cu, \text{ or } Zn$). Accurate unit cell dimensions have been obtained from Guinier-Hägg photographic X-ray diffraction data. The cell volumes of the $(Ni_{1-z}Me_z)_3(PO_4)_2$ phases are correlated to the size and amount of Me^{2+} . Rietveld full-profile refinements based on neutron powder diffraction data have been utilized to determine the distribution of cations among the two distinct octahedral sites M1 and M2. The preference for M1 over M2 is



The cation distribution results are compared with corresponding results for olivines, orthopyroxenes, and some other oxosalt structures with metal-oxygen octahedra similar in size and shape to those in olivine. It is concluded that the Ni^{2+}/Me^{2+} distributions in these structure types are mainly controlled by crystal field energies, while the size effects are small.

Introduction

Many cation distribution studies of oxosalt solid solutions have been published during the last 25 years, principally concerning divalent-metal cations ubiquitous in nature such as $Mg^{2+}, Fe^{2+}, Mn^{2+}, Zn^{2+}, Ca^{2+}$ etc. Such investigations are of great importance not only to mineralogists and geochemists, but also to inorganic chemists. Within this field I have earlier performed systematic studies involving five- and six-coordinated environments of oxygen atoms (cf. Nord and Stefanidis, 1981; Nord and Ericsson,

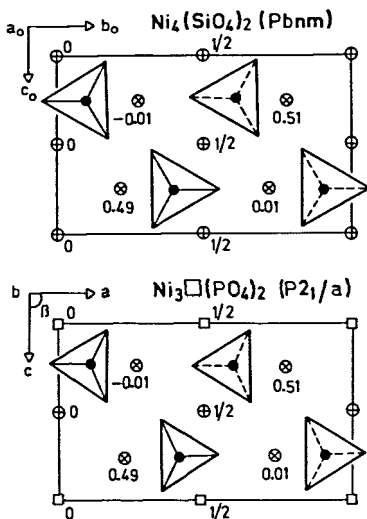


Fig. 1. Schematic drawings of the olivine and sarcopside structures, here represented by $Ni_4(SiO_4)_2$ (Lager and Meagher, 1978) and $Ni_3\square(PO_4)_2$ (Calvo and Faggiani, 1975). Symbols: $\oplus = M1$, $\otimes = M2$, $\square =$ "M3" vacancy; filled circles represent Si or P. Approximate coordinates for the a_0 and b axes are given

1982). Most cation distribution studies, though, concern important rock-forming minerals like *olivine*, but some of these results are contradictory (cf. Brown, 1980; Nover and Will, 1981). Further systematic studies of olivines and olivine-related phases are therefore desirable to help clarify these complicated matters.

Several non-silicate minerals crystallize with the olivine structure type, e.g. *chrysoberyl* (Al_2BeO_4), *sinhalite* ($AlMgBO_4$), and *triflylite* ($LiFePO_4$). In addition, Moore (1972) has shown that *sarcopside*, $(Fe,Mn,Mg)_3(PO_4)_2$ (Websky, 1868), is structurally related to olivine. Nickel orthophosphate is isotypic with sarcopside (Calvo and Faggiani, 1975), and the same is true for some other orthophosphates (see below). Like olivine, they all contain Me^{2+} cations. For these reasons and because numerous sarcopside-type phases may be prepared, they are suitable for cation distribution studies.

The close structural relationship between the olivine Ni_2SiO_4 (Lager and Meagher, 1978) and $Ni_3(PO_4)_2$ -sarcopside (Calvo and Faggiani, 1975) is illustrated in Figure 1. Olivine, for convenience here denoted $M_4(SiO_4)_2$, is orthorhombic ($Pbnm$) with two four-fold, six-coordinated M^{2+} sites, here called $M1_{ol}$ and $M2_{ol}$ (point symmetries: $\bar{1}$ and m). In sarcopside, here denoted $M_3\square(PO_4)_2$, the symmetry has been lowered to monoclinic ($P2_1/a$; $\beta \approx 91^\circ$). The four $M1_{ol}$ "olivine" sites in the unit cell have been split into a two-fold site $M1$ (0,0,1/2 and 1/2,1/2,1/2) and another two-fold site $M3$, or

"□", vacant in $\text{Ni}_3\text{□}(\text{PO}_4)_2$ (0,0,0 and 1/2,1/2,0), while the four-fold $M2_{01}$ sites are preserved as M2. All sites (also M3) are octahedrally coordinated. M1 and M2 have the point symmetries $\bar{1}$ and 1, respectively. In both structures the "(M2)O₆" octahedra are slightly larger and display a somewhat larger scatter in metal–oxygen distances and O–M–O angles than "(M1)O₆". ["(M3)O₆" is considerably larger.] All atoms, including the oxygens, occupy corresponding positions in the two structures (cf. Fig. 1). The respective unit cell lengths are also very similar: $a_0/b = 1.006$, $b_0/a = 1.001$, and $c_0/c = 1.014$. Naturally there are some slight structural differences, e.g. the P–O distances are about 0.1 Å shorter than the corresponding Si–O distances.

The present paper reports on X-ray and neutron diffraction studies of $(\text{Ni}_{1-z}\text{Me}_z)_3(\text{PO}_4)_2$ sarcopside-type solid solutions, henceforward abbreviated Ni/Me (*Me* = Mg, Mn, Fe, Co, Cu, or Zn). Some results earlier obtained will be included in the discussions, which mainly concern unit cell dimensions, solubility ranges, and cation distributions. A comparison with olivines, orthopyroxenes, and some other oxosalt structures will also be made.

Experimental procedures

Pure orthophosphates were synthesized by heating the respective metal oxide with ammonium dihydrogen phosphate at 1200 K. In total about 60 various $(\text{Ni}_{1-z}\text{Me}_z)_3(\text{PO}_4)_2$ solid solutions were then prepared and equilibrated at 1070 K (cf. Nord and Ericsson, 1982). Accurate X-ray powder diffraction data of each sample were obtained at 295 K with an XDC-700 type focusing camera (monochromatized $\text{CrK}\alpha_1$ radiation, $\lambda = 2.28975$ Å; KCl internal standard). Some phases were also analysed with an energy-dispersive EDAX unit attached to a JEOL JSM-35 scanning electron microscope.

Three samples were selected for further neutron diffraction studies with the basic aim to determine the cation partitionings: $(\text{Ni}_{0.65}\text{Co}_{0.35})_3(\text{PO}_4)_2$, $(\text{Ni}_{0.35}\text{Co}_{0.65})_3(\text{PO}_4)_2$, and $(\text{Ni}_{0.70}\text{Mn}_{0.30})_3(\text{PO}_4)_2$. About 10 g each of these compositions were prepared. Neutron powder diffraction data of the first phase were collected at the 2 MW JEEP-2 reactor at Kjeller, Norway, using a "squashed" germanium monochromator crystal ($\lambda \approx 1.882$ Å, $\Delta\theta = 0.025^\circ$). Data for the two other samples were collected at the Studsvik R2 reactor (Studsvik, Nyköping, Sweden), using double monochromators (copper crystals) in parallel setting ($\lambda \approx 1.550$ Å, $\Delta\theta = 0.040^\circ$).

Unit cell dimensions

The internal standard (KCl) reflections were used to correct the visual readings of the Guinier-Hägg photographs, and the unit cell dimensions ($P2_1/a$, $Z = 2$) were refined with a least-squares procedure from 25–30

unambiguously indexed reflections (programs LAZY and CELREF by A. G. Nord). The cell parameters of the $(\text{Ni}_{1-z}\text{Me}_z)_3(\text{PO}_4)_2$ sarcopside phases ($\text{Me} = \text{Cu}, \text{Co}, \text{Zn}, \text{Fe}, \text{Mn}$) are listed in Table 1, which also indicates the approximate homogeneity regions. The cell volumes, also for Ni/Mg

Table 1. Unit cell dimensions ($P2_1/a$) at 295 K for some $(\text{Ni}_{1-z}\text{Me}_z)_3(\text{PO}_4)_2$ sarcopside-type solid solutions, equilibrated at 1070 K. Data for some pure $\text{Me}_3(\text{PO}_4)_2$ -sarcopsides are also included. Data for the Ni,Mg-phases have earlier been published (Nord and Stefanidis, 1983)

<i>Me</i>	<i>z</i>	<i>a</i> (Å)	<i>b</i> (Å)	<i>c</i> (Å)	β (°)	<i>V</i> (Å ³)
Ni	0 ^a	10.108(2)	4.698(1)	5.831(1)	91.12(2)	276.8(1)
Mg	1 ^b	10.25(2)	4.72(1)	5.92(1)	90.9(1)	287(1)
Cu	0.05	10.105(2)	4.698(1)	5.844(2)	91.10(3)	277.4(2)
Co	0.05 ^c	10.112(3)	4.697(2)	5.832(2)	91.11(3)	277.0(3)
	0.10 ^c	10.113(2)	4.698(1)	5.832(1)	91.10(2)	277.0(2)
	0.15 ^c	10.117(2)	4.698(1)	5.831(2)	91.13(2)	277.1(2)
	0.20 ^c	10.120(3)	4.697(1)	5.832(1)	91.15(2)	277.2(2)
	0.30	10.174(4)	4.709(2)	5.862(2)	91.14(3)	280.8(3)
	0.33	10.182(3)	4.711(2)	5.864(3)	91.12(3)	281.2(3)
	0.35	10.185(4)	4.713(3)	5.865(2)	91.09(3)	281.5(3)
	0.40	10.217(5)	4.717(4)	5.864(5)	91.15(5)	282.5(5)
	0.45	10.219(3)	4.718(2)	5.872(3)	91.12(3)	283.0(3)
	0.50	10.221(2)	4.719(1)	5.879(2)	91.07(2)	283.5(2)
	0.55	10.233(3)	4.721(3)	5.880(2)	91.18(3)	284.1(3)
	0.60	10.243(3)	4.723(3)	5.888(2)	91.12(3)	284.8(3)
	0.65	10.247(3)	4.728(2)	5.889(2)	91.07(3)	285.3(3)
	0.67	10.254(3)	4.729(2)	5.892(2)	91.13(2)	285.6(3)
	1 ^d	10.33(3)	4.75(2)	5.92(2)	91.1(1)	290(1)
Zn	0.10	10.118(3)	4.699(2)	5.835(1)	91.11(2)	277.4(2)
	0.15	10.127(3)	4.703(2)	5.847(2)	91.12(2)	278.4(3)
	0.20	10.136(4)	4.704(1)	5.860(2)	91.16(3)	279.3(3)
	0.25	10.144(3)	4.706(2)	5.864(2)	91.14(2)	279.9(2)
	0.30	10.150(2)	4.707(1)	5.870(1)	91.11(2)	280.4(1)
	0.33	10.155(2)	4.710(2)	5.872(3)	91.12(3)	280.8(3)
Fe	0.10	10.145(2)	4.700(1)	5.858(1)	91.06(2)	279.3(1)
	0.20	10.186(2)	4.703(2)	5.882(1)	91.02(3)	281.7(2)
	0.30	10.220(2)	4.707(1)	5.908(1)	91.00(1)	284.2(1)
	0.40	10.267(2)	4.712(1)	5.933(1)	90.97(2)	287.0(1)
	0.50	10.306(3)	4.717(1)	5.959(2)	90.92(2)	289.6(2)
	0.60	10.350(2)	4.724(2)	5.984(2)	90.89(3)	292.5(3)
	0.67	10.363(3)	4.732(1)	5.990(1)	90.91(2)	293.7(2)
	0.70	10.368(3)	4.735(2)	5.994(1)	90.92(2)	294.2(3)

Table 1. (Continued)

<i>Me</i>	<i>z</i>	<i>a</i> (Å)	<i>b</i> (Å)	<i>c</i> (Å)	β (°)	<i>V</i> (Å ³)
	1 ^c	10.442(3)	4.787(1)	6.029(1)	90.97(2)	301.3(2)
Mn	0.05	10.110(1)	4.697(1)	5.833(1)	91.15(1)	276.9(1)
	0.10	10.133(5)	4.717(4)	5.850(3)	90.55(4)	279.6(5)
	0.15	10.158(4)	4.724(3)	5.867(3)	90.62(4)	281.6(4)
	0.20	10.185(5)	4.734(5)	5.886(4)	90.61(5)	283.8(5)
	0.25	10.224(4)	4.730(3)	5.922(2)	90.74(2)	286.3(3)
	0.30	10.267(3)	4.726(1)	5.961(1)	90.82(2)	289.2(3)

^a Ni₃(PO₄)₂ (Nord and Stefanidis, 1983)

^b High-pressure sarcopside phase of magnesium orthophosphate (Annersten and Nord, 1980)

^c Although sarcopside-related, these phases may have a space group symmetry other than *P*2₁/*a*

^d Metastable phase Co₃□(PO₄)₂ (Berthet et al., 1972)

^e Hydrothermally prepared Fe₃(PO₄)₂-sarcopside (Ericsson and Nord, 1984)

(Nord and Stefanidis, 1983), are plotted versus composition in Figure 2. The Ni/*Me* series will be discussed in order of increasing *Me*²⁺ cation radius, *r*_{*Me*}, as reported by Shannon and Prewitt (1969) for an octahedral environment of oxygen atoms (*r*_{Ni} = 0.70 Å). Unless specified, all data refer to samples equilibrated at 1070 K, 1 bar, which are thermodynamically stable at room temperature.

The results for the (Ni_{1-*z*}Mg_{*z*})₃(PO₄)₂ series (Nord and Stefanidis, 1983) will be briefly summarized (*r*_{Mg} = 0.72 Å). There are two monophasic regions, "I" (0 ≤ *z* ≤ 0.27) and "II" (0.40 ≤ *z* ≤ 0.60); between them a small two-phase region (see Fig. 2). This anomaly will be further discussed below. A metastable Mg-sarcopside has been prepared by Berthet et al. (1972); it is usually denoted Mg₃□(PO₄)₂ to distinguish it from the "ordinary" farringtonite-type Mg₃(PO₄)₂ which has five- and six-coordinated cations (Nord and Kierkegaard, 1968). Mg₃□(PO₄)₂ has later been identified as a high-pressure phase (Annersten and Nord, 1980). Its unit cell volume is 287 Å³; the extrapolated dashed line for the "region II" phases passes through this point (at *z* = 1 in Fig. 2).

The solubility of Cu₃(PO₄)₂ in Ni₃(PO₄)₂ is low, only about 5 mole % (*r*_{Cu} = 0.73 Å). The Ni/Co series (*r*_{Co} = 0.74 Å) resembles Ni/Mg, with two "regions" and a discontinuity in the *V* = *f*(*z*) curve. Again a metastable Co₃□(PO₄)₂ phase exists (cf. Table 1 and Fig. 2). There seems to be yet another slight anomaly among the region II Ni/Co phases, with a small discontinuity in *V* = *f*(*z*) somewhere between 0.35 and 0.40 for *z*. Since the drawing of the region II graph may be controversial, it has been omitted in Fig. 2. It is clear, though, that the extrapolated line in question must pass very near the point for pure Co-sarcopside (*V* = 290 Å³, *z* = 1). The solubility of

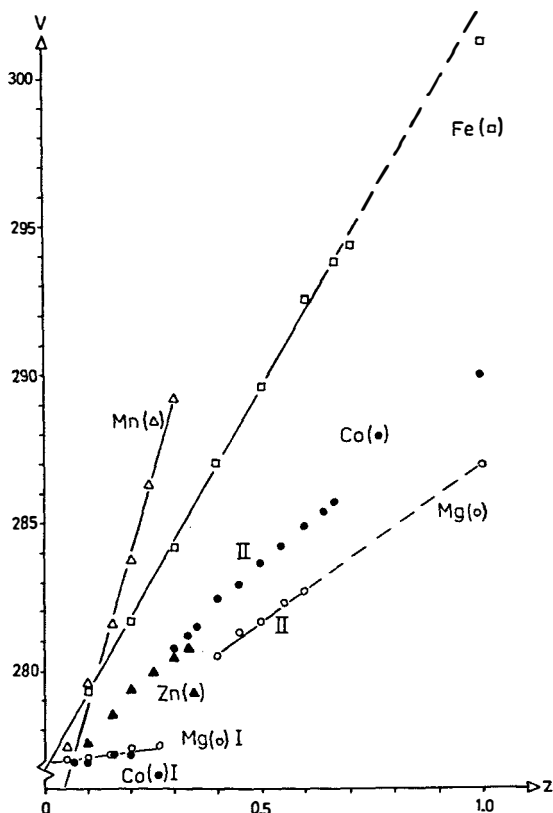


Fig. 2. Unit cell volumes V (in \AA^3) versus composition z for some $(\text{Ni}_{1-z}\text{Me}_z)_3(\text{PO}_4)_2$ sarcopside-type solid solutions. The values at $z = 1$ refer to high-pressure modifications (see text); all other phases have been equilibrated at 1070 K, 1 bar. For clarity, $(\text{Ni}_{0.95}\text{Cu}_{0.05})_3(\text{PO}_4)_2$, with $V = 277.4 \text{\AA}^3$, has not been included

zinc ($r_{\text{Zn}} = 0.75 \text{\AA}$) is about 33%. The solubility of Fe^{2+} ($r_{\text{Fe}} = 0.77 \text{\AA}$) is surprisingly large, about 70%. The extrapolated $V = f(z)$ graph for the Ni/Fe series passes slightly above the observed value (at $z = 1$) for pure Fe-sarcopside, hydrothermally prepared as described by Mattievich and Danon (1977), and crystallographically analysed by Ericsson and Nord (1984). [Usually, $\text{Fe}_3(\text{PO}_4)_2$ crystallizes with the graptolite structure, with 5,5,6-coordinated cations (Kostiner and Rea, 1974).] Mn^{2+} is the largest cation involved in this study ($r_{\text{Mn}} = 0.82 \text{\AA}$). Cd^{2+} (0.95 \AA) and Ca^{2+} (1.00 \AA) were not incorporated in pure $\text{Ni}_3(\text{PO}_4)_2$ at 1070 K, they are probably too large.

Disregarding some slight anomalies, the $V = f(z)$ graphs of the Ni/Me series are usually linear and passes through or near the point for pure nickel orthophosphate ($V = 276.8 \text{\AA}^3$ at $z = 0$). However, the Ni/Mn graph in-

Table 2. Data for the $(\text{Ni}_{1-z}\text{Me}_z)_3(\text{PO}_4)_2$ solid solutions (1070 K, 1 bar). The cation radii, r_{Me} , are from Shannon and Prewitt (1969). ($r_{\text{Ni}} = 0.70 \text{ \AA}$.) Abbreviations: $V' = \Delta V/\Delta z$, $Z = 2$, $\Delta r = r_{\text{Me}} - r_{\text{Ni}}$. The values for Ni/Mg are taken from Nord and Stefanidis (1983)

<i>Me</i>	r_{Me} (Å)	Homogeneity range (%)		V' (Å ³)	$V'/(Z \cdot \Delta r)$
Mg	0.72	Region I	0–27	3	70
		Region II	40–60	9	230
Cu	0.73		0–5	12	200
		Region I	0–20	2	25
Co	0.74	Region II	30–67	13	160
			0–33	12	130
Zn	0.75		0–70	25	180
Fe	0.77		0–30	49	200
Mn	0.82		0		
Cd	0.95		0		
Ca	1.00		0		

tercepts the V axis at $V \approx 274 \text{ \AA}^3$. Although this might indicate a slight structural anomaly, the successful refinement of the solid solution $(\text{Ni}_{0.70}\text{Mn}_{0.30})_3(\text{PO}_4)_2$ does not support this idea (see next section). The individual unit cell axis lengths also change almost linearly with the composition. Within each Ni/*Me* series, the smallest variation is noted for the monoclinic b axis. This is noteworthy, because in practically all $(\text{ME}_{1-z}\text{Me}_z)_3(\text{PO}_4)_2$ farringtonite and graftonite series, with the same space group symmetry as sarcopside, the largest change with composition was observed for the b axis (Nord and Stefanidis, 1981; Nord and Ericsson, 1982). (*ME* and *Me* are divalent metals).

In the above mentioned studies of farringtonite and graftonite phases, the variation in unit cell volume has been quantified by means of the derivative $V' = \Delta V/\Delta z$ for the respective $V = f(z)$ graph of the $(\text{ME}_{1-z}\text{Me}_z)_3(\text{PO}_4)_2$ series, and by the ratio $V'/(Z \cdot \Delta r)$, where Z is the number of formula units per unit cell, and $\Delta r = r_{\text{ME}} - r_{\text{Me}}$. The latter ratio was found to be fairly constant within each structure group. Corresponding values for the Ni/*Me* series are given in Table 2. These results clearly show that the unit cell volume of a Ni/*Me* phase is correlated to the degree of Me^{2+} substitution, and to the cationic radius. The "regions I" of Ni/Mg and Ni/Co, though, are exceptional, with significantly lower $V'/(Z \cdot \Delta r)$ values than the average value ($\sim 150 \text{ \AA}^2$), suggesting a slight structural anomaly with regard to sarcopside, which has been verified for the phase $(\text{Ni}_{0.73}\text{Mg}_{0.27})_3(\text{PO}_4)_2$ (Nord and Stefanidis, 1983). A similar anomaly at 1070 K is likely to prevail for the "region I" Ni/Co phases, although this has not been verified.

Neutron diffraction studies

Neutron powder diffraction studies of three sarcopside phases have been undertaken with the basic aim to determine the cation partitioning, namely in

$(\text{Ni}_{0.65}\text{Co}_{0.35})_3(\text{PO}_4)_2$, $(\text{Ni}_{0.35}\text{Co}_{0.65})_3(\text{PO}_4)_2$, and $(\text{Ni}_{0.70}\text{Mn}_{0.30})_3(\text{PO}_4)_2$. The neutron scattering amplitudes are unusually favourable: $b(\text{Ni}) = +1.03$, $b(\text{Co}) = +0.25$, and $b(\text{Mn}) = -0.36$ (all in 10^{-12} cm units). Since the technique has already been described in detail (Nord, 1982), it is only briefly outlined below.

$(\text{Ni}_{0.65}\text{Co}_{0.35})_3(\text{PO}_4)_2$ was investigated first. The neutron intensity profile ($3 \leq \theta \leq 38.5^\circ$, $\lambda \approx 1.882 \text{ \AA}$) contained 80 independent, partly overlapping Bragg reflections. After subtraction of the graphically determined background, the net intensities were processed by means of the Rietveld (1969) full-profile refinement technique. After some trial refinements, the complete structure ($P2_1/a$) was refined with 25 parameters: one scale factor, three profile parameters to define the Gaussian shape of the peaks, 18 atomic positional parameters, and three isotropic temperature factors (for the metal, phosphorus, and oxygen atoms). In lieu of refining constrained occupancy factors for the metals, which anyway necessitates approximately known starting values, the cation distribution was determined through a series of refinements with a systematically shifted distribution parameter x , defined by the expression

$$(\text{Ni}_{1-2x}\text{Co}_{2x})^{\text{M}1}(\text{Ni}_{0.475+x}\text{Co}_{0.525-x})_2^{\text{M}2}(\text{PO}_4)_2 \quad (0 \leq x \leq 0.50).$$

This technique gives more reasonable temperature factors and smaller correlations between refined parameters than a conventional refinement of occupancy factors. The fact that one of the metals (Mn) has a negative scattering amplitude is another reason to avoid the refinement of occupancy factors.

The refinement results, displayed as $R_1 = f(x)$, are shown in Figure 3. A minimum R_1 was found at $x = 0.13 \pm 0.02$, with $R_1 = 0.056$ and $R_p = 0.11$. ($R_1 = \Sigma |I_{\text{obs}} - I_{\text{calc}}| / \Sigma I_{\text{obs}}$ for integrated reflection intensities). Since $x = 0.175$ defines a random distribution, the present result indicates a slight partial ordering of nickel at the M1 sites.

$(\text{Ni}_{0.35}\text{Co}_{0.65})_3(\text{PO}_4)_2$ was then refined in a similar way. Because of a shorter wavelength ($\sim 1.550 \text{ \AA}$), the intensity profile now contained 175 independent reflections ($3 \leq \theta \leq 40.3^\circ$). The cation distribution parameter was defined by

$$(\text{Ni}_{1-2x}\text{Co}_{2x})^{\text{M}1}(\text{Ni}_{0.025+x}\text{Co}_{0.975-x})_2^{\text{M}2}(\text{PO}_4)_2 \quad (0 \leq x \leq 0.50).$$

Note that x has now a different meaning compared with the former phase: $x = 0.325$ now represents a random distribution of the cations, while $x < 0.325$ means that nickel is partially ordered at M1. The lowest R_1 value, 0.044 ($R_p = 0.08$), was obtained for $x = 0.27 \pm 0.01$ (cf. Fig. 3).

$(\text{Ni}_{0.70}\text{Mn}_{0.30})_3(\text{PO}_4)_2$ was finally refined (142 independent reflections, $\lambda \approx 1.550 \text{ \AA}$, $3 \leq \theta \leq 37.5^\circ$), defined as

$$(\text{Ni}_{1-2x}\text{Mn}_{2x})^{\text{M}1}(\text{Ni}_{0.55+x}\text{Mn}_{0.45-x})_2^{\text{M}2}(\text{PO}_4)_2 \quad (0 \leq x \leq 0.45).$$

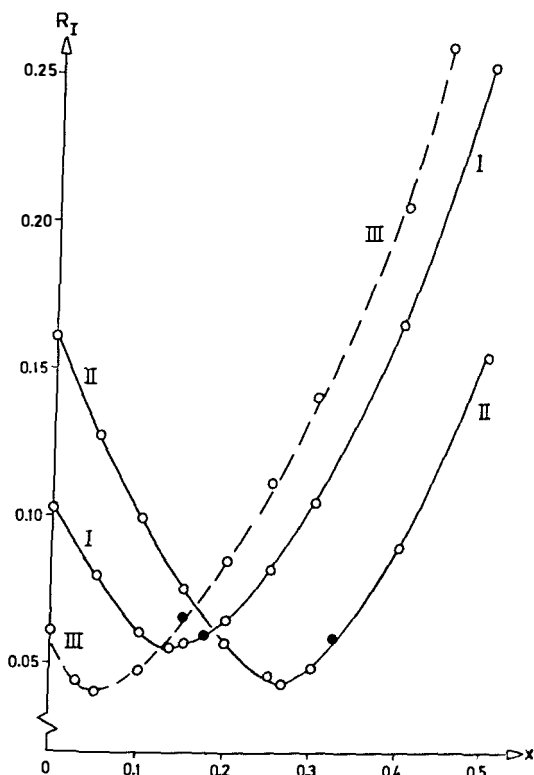


Fig. 3. R_I values versus the cation distribution parameter x (compare text) for the profile-refinements of the sarcopside phases I = $(\text{Ni}_{0.65}\text{Co}_{0.35})_3(\text{PO}_4)_2$, II = $(\text{Ni}_{0.35}\text{Co}_{0.65})_3(\text{PO}_4)_2$, and III = $(\text{Ni}_{0.70}\text{Mn}_{0.30})_3(\text{PO}_4)_2$. ● = random distribution, ○ = partial ordering of the cations

A minimum was located at $x = 0.05 \pm 0.01$ (random at $x = 0.15$), with $R_I = 0.041$, $R_p = 0.08$. The atomic parameters for the three phases are given in Table 3. All atoms are labelled in accordance with the generally adopted olivine nomenclature. The observed and calculated intensity profiles for one of the refinements is shown in Figure 4.

Discussion

Like the olivine structure, the sarcopside structure consists of hexagonally close-packed layers of oxygen atoms. In olivine, the rather regular MO_6 octahedra are connected in serrated chains; sarcopside contains trimers of edge-sharing, distorted MO_6 octahedra (Moore, 1972), cf. Figures 1 and 5. Some interatomic distances and angles for the three profile-refined Ni/Me-sarcopsides are given in Table 4. For comparison, some selected values have

Table 3. Atomic parameters for the three profile-refined sarcopside-type solid solutions (neutron diffraction data). Space group $P2_1/a$

Atom		$\text{Ni}_{0.65}\text{Co}_{0.35}$ ^a	$\text{Ni}_{0.35}\text{Co}_{0.65}$ ^b	$\text{Ni}_{0.70}\text{Mn}_{0.30}$ ^c
M1	x	0	0	0
	y	0	0	0
	z	1/2	1/2	1/2
M2	x	0.279(1)	0.275(1)	0.279(1)
	y	-0.006(2)	-0.003(2)	-0.015(2)
	z	0.244(1)	0.243(1)	0.241(1)
P	x	0.087(1)	0.093(1)	0.095(1)
	y	0.428(2)	0.421(1)	0.422(2)
	z	0.254(2)	0.255(1)	0.259(1)
O1	x	0.100(1)	0.105(1)	0.099(1)
	y	0.750(2)	0.746(1)	0.751(2)
	z	0.277(2)	0.270(1)	0.271(2)
O2	x	0.458(1)	0.459(1)	0.459(1)
	y	0.194(2)	0.192(1)	0.194(1)
	z	0.261(2)	0.255(2)	0.259(2)
O3	x	0.176(1)	0.179(1)	0.170(1)
	y	0.313(2)	0.314(1)	0.304(2)
	z	0.050(2)	0.055(1)	0.064(2)
O4	x	0.156(1)	0.164(1)	0.161(1)
	y	0.273(2)	0.271(1)	0.268(2)
	z	0.463(2)	0.472(1)	0.471(1)
$B(\text{M})[\text{Å}^2]$		1.4(1)	0.8(2)	-0.1(1)
$B(\text{P})[\text{Å}^2]$		0.7(3)	0.3(1)	0.1(2)
$B(\text{O})[\text{Å}^2]$		0.9(2)	0.4(1)	0.4(1)

^a $(\text{Ni}_{0.65}\text{Co}_{0.35})_3(\text{PO}_4)_2$ ^b $(\text{Ni}_{0.35}\text{Co}_{0.65})_3(\text{PO}_4)_2$ ^c $(\text{Ni}_{0.70}\text{Mn}_{0.30})_3(\text{PO}_4)_2$

been summarized in Table 5 for the here and earlier studied Ni/Me phases. Results on $\text{Ni}_3(\text{PO}_4)_2$ from a single-crystal study (Calvo and Faggiani, 1975) and from a profile-refinement based on X-ray Guinier-Hägg powder diffraction data (Nord and Stefanidis, 1983) are included so that the reader may judge the accuracy of the Rietveld method applied on the sarcopside structure.

Cation distributions in $(\text{Ni,Me})_3(\text{PO}_4)_2$ sarcopsides

In the sarcopside structure ($P2_1/a$), M1 and M2 have point symmetries $\bar{1}$ and 1, respectively. Moreover, $(\text{M2})\text{O}_6$ is somewhat more distorted than $(\text{M1})\text{O}_6$, with a larger scatter in the metal-oxygen distances and the

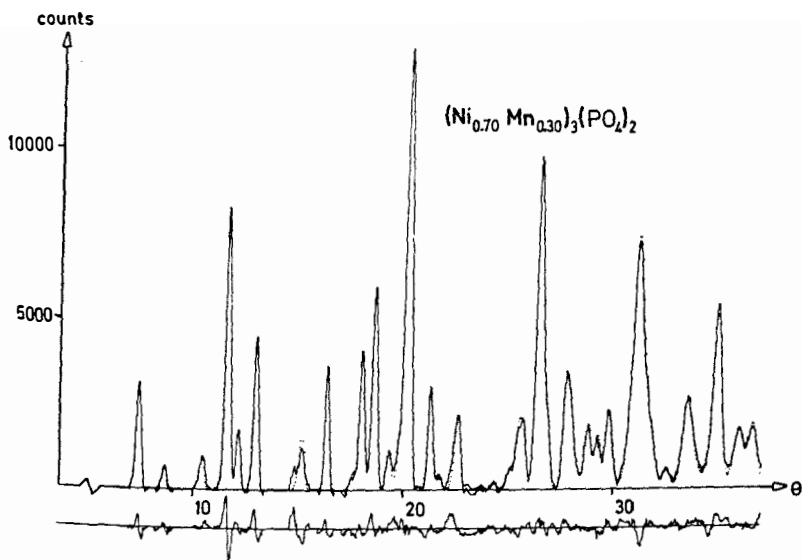


Fig. 4. The least-squares fit obtained between the observed intensities (solid line) and calculated intensities (points) from the final Rietveld refinement of $(\text{Ni}_{0.70}\text{Mn}_{0.30})_3(\text{PO}_4)_2$ (neutron diffraction data). The discrepancy in the fit, defined as $I_{\text{obs}} - I_{\text{calc}}$, is plotted below to the same scale

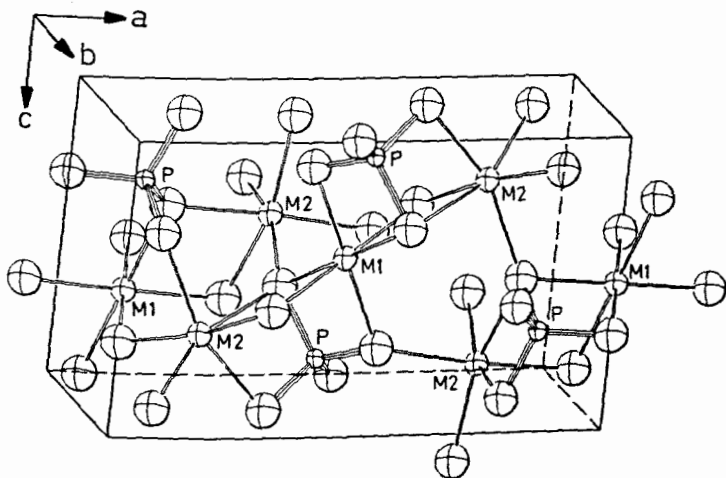
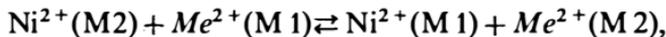


Fig. 5. An ORTEP (Johnson, 1965) illustration of the sarcopside structure ($P2_1/a$), showing an M2-M1-M2 trimer of edge-sharing MO_6 octahedra

Table 4. Interatomic distances (Å) and angles (°) in $(\text{Ni}_{0.65}\text{Co}_{0.35})_3(\text{PO}_4)_2$, $(\text{Ni}_{0.35}\text{Co}_{0.65})_3(\text{PO}_4)_2$ and $(\text{Ni}_{0.70}\text{Mn}_{0.30})_3(\text{PO}_4)_2$. The standard deviations of the O–P–O angles is $\pm 0.8^\circ$ or less

Distances	$(\text{Ni}_{0.65}\text{Co}_{0.35})_3(\text{PO}_4)_2$	$(\text{Ni}_{0.35}\text{Co}_{0.65})_3(\text{PO}_4)_2$	$(\text{Ni}_{0.70}\text{Mn}_{0.30})_3(\text{PO}_4)_2$
M 1–O 1 (x2)	2.05(1)	2.11(1)	2.08(1)
M 1–O 2 (x2)	2.06(1)	2.08(1)	2.07(1)
M 1–O 4 (x2)	2.06(1)	2.12(1)	2.09(1)
Average	2.06	2.10	2.08
M 2–O 1	2.16(2)	2.12(2)	2.15(2)
M 2–O 2	2.05(2)	2.09(2)	2.10(2)
M 2–O 3	2.14(2)	2.10(2)	2.14(2)
M 2–O 3'	1.99(2)	2.02(2)	2.08(2)
M 2–O 4	2.24(2)	2.20(2)	2.27(2)
M 2–O 4'	2.10(2)	2.08(2)	2.09(2)
Average	2.11	2.10	2.14
P–O 1	1.52(2)	1.54(2)	1.56(2)
P–O 2	1.45(2)	1.47(2)	1.50(2)
P–O 3	1.59(2)	1.57(2)	1.51(2)
P–O 4	1.58(2)	1.61(2)	1.59(2)
Average	1.54	1.55	1.54
O 1–P–O 2	117.9	115.9	112.8
O 1–P–O 3	110.8	108.7	112.9
O 1–P–O 4	110.8	110.8	114.1
O 2–P–O 3	114.5	114.7	110.6
O 2–P–O 4	100.5	104.1	102.3
O 3–P–O 4	100.3	101.5	103.2
Average	109.2	109.3	109.3

O–M–O angles; the average M 1–O and M 2–O distances are very similar (cf. Tables 5 and 6). The $\text{Ni}^{2+}/\text{Me}^{2+}$ distribution among M 1 and M 2 in sarcopside is conventionally defined as in olivine by a distribution coefficient K_D . This may be regarded as the equilibrium constant at the temperature in question (here: 1070 K) for the cation exchange reaction



assuming equal activity factors. Thus:

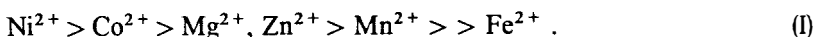
$$K_D(\text{Ni}, \text{Me}) = [\text{X}_{\text{Ni}}(\text{M}1) \cdot \text{X}_{\text{Me}}(\text{M}2)] / [\text{X}_{\text{Ni}}(\text{M}2) \cdot \text{X}_{\text{Me}}(\text{M}1)].$$

Note that a random distribution of the cations is characterized by $K_D = 1$, while $K_D > 1$ indicates that Ni^{2+} has a greater tendency for M 1 than has Me^{2+} . In the solid solutions refined in the present study, the results show that $K_D(\text{Ni}, \text{Co})$ is 1.9 ± 0.3 in $(\text{Ni}_{0.65}\text{Co}_{0.35})_3(\text{PO}_4)_2$ and 2.0 ± 0.1 in $(\text{Ni}_{0.35}\text{Co}_{0.65})_3(\text{PO}_4)_2$, while $K_D(\text{Ni}, \text{Mn}) = 6 \pm 1$ in $(\text{Ni}_{0.70}\text{Mn}_{0.30})_3(\text{PO}_4)_2$.

Table 5. Interatomic distances (average values and distance ranges in Å units) for the $(\text{Ni}_{1-z}\text{Me}_z)_3(\text{PO}_4)_2$ sarcopside structures ($P2_1/a$). XSC = X-ray single-crystal study, XPD = X-ray powder diffraction, NPD = neutron powder diffraction

Compound	Reference	M 1 – O distances		M 2 – O distances		P – O distances		
		Average	Range	Average	Range	Average	Range	
$\text{Ni}_3(\text{PO}_4)_2$	Calvo and Faggiani, 1975	2.081	2.07–2.10	2.084	2.00–2.19	1.547	1.52–1.60	XSC
$(\text{Ni}_{0.60}\text{Mg}_{0.40})_3(\text{PO}_4)_2$	Nord and Stefanidis, 1983	2.14	2.12–2.16	2.08	2.02–2.17	1.52	1.46–1.56	XPD
$(\text{Ni}_{0.45}\text{Mg}_{0.55})_3(\text{PO}_4)_2$	Nord and Stefanidis, 1983	2.15	2.13–2.19	2.09	2.02–2.14	1.53	1.47–1.59	XPD
$\text{Ni}_3(\text{PO}_4)_2$	Nord and Stefanidis, 1983	2.08	2.05–2.13	2.10	1.98–2.20	1.53	1.46–1.59	XPD
$(\text{Ni}_{0.65}\text{Co}_{0.35})_3(\text{PO}_4)_2$	This work	2.06	2.05–2.06	2.11	1.99–2.24	1.54	1.45–1.59	NPD
$(\text{Ni}_{0.35}\text{Co}_{0.65})_3(\text{PO}_4)_2$	This work	2.10	2.08–2.12	2.10	2.02–2.20	1.55	1.47–1.61	NPD
$(\text{Ni}_{0.75}\text{Zn}_{0.25})_3(\text{PO}_4)_2$	Nord, 1982	2.09	2.08–2.10	2.10	1.98–2.25	1.54	1.48–1.60	NPD
$\text{NiFe}_2(\text{PO}_4)_2$	Ericsson and Nord, 1984	2.11	2.10–2.12	2.15	2.01–2.37	1.54	1.47–1.58	NPD
$(\text{Ni}_{0.70}\text{Mn}_{0.30})_3(\text{PO}_4)_2$	This work	2.08	2.07–2.09	2.14	2.08–2.27	1.54	1.50–1.59	NPD

In earlier studied Ni/Me phases, also equilibrated at 1070 K, K_D values have been obtained for Ni/Zn, Ni/Mg, and Ni/Fe (see Table 6). The cations studied so far may thus be arranged in the following sequence with respect to their preference for M1 over M2 in the sarcopside structure:



The cation distribution patterns in the Ni/Me-sarcopsides are usually well correlated with the observed changes in averaged metal-oxygen distances with respect to the "reference" structure $\text{Ni}_3(\text{PO}_4)_2$. This will be exemplified for $(\text{Ni}_{0.70}\text{Mn}_{0.30})_3(\text{PO}_4)_2$. In this phase the average M2-O distance has increased by about 0.056 Å with respect to nickel orthophosphate, while the M1-O mean distance is almost unchanged. This effect is caused by replacing 30% of the nickel ions by larger Mn^{2+} ions in an ordered way, expressed from the refinement results by the formula $(\text{Ni}_{0.90}\text{Mn}_{0.10})^{\text{M1}}(\text{Ni}_{0.60}\text{Mn}_{0.40})^{\text{M2}}(\text{PO}_4)_2$. With the Shannon-Prewitt (1969) cation radii, the calculated increase with respect to $\text{Ni}_3(\text{PO}_4)_2$ for the average M2-O would be $(0.60 \cdot r_{\text{Ni}} + 0.40 \cdot r_{\text{Mn}}) - r_{\text{Ni}} \approx 0.05 \text{ \AA}$. For M1-O the corresponding calculated increase is $\sim 0.01 \text{ \AA}$, so both these concepts agree well with the observed changes.

The farringtonite-type solid solutions display good correlation between homogeneity ranges and cation distributions (Nord and Stefanidis, 1981). Among the Ni/Me-sarcopsides there is no such obvious relationship except for the Ni/Fe series: the strong preference of Fe^{2+} for the more numerous M2 sites ($\sim 67\%$ of all available sites) accords with the maximum solubility of 70% $\text{Fe}_3(\text{PO}_4)_2$ in $\text{Ni}_3(\text{PO}_4)_2$.

Partitioning of $\text{Ni}^{2+}/\text{Me}^{2+}$ in the olivine structure

The "M1" and "M2" sites in olivine (*Pbnm*) have point symmetries $\bar{1}$ and *m*. In Ni_2SiO_4 , (M2) O_6 is somewhat larger and slightly more distorted than (M1) O_6 (Lager and Meagher, 1978), see Table 6. Unfortunately, the number of (Ni,Me) $_2\text{SiO}_4$ olivines that have been investigated crystallographically is very limited. A naturally occurring nickel-rich olivine (*liebenbergite* from Barberton, South Africa) has been studied by Bish (1981), showing that nickel is strongly ordered at the M1 sites. $K_D(\text{Ni,Me})$ values for some synthetic (Ni,Me) $_2\text{SiO}_4$ olivines are summarized in Table 6. To my knowledge no other Ni,Me-olivines have been analysed with the aim to determine $K_D(\text{Ni,Me})$. However, since K_D may be regarded as the equilibrium constant of the respective cation exchange reaction, further values may be roughly estimated from the relation

$$K_D(\text{Ni,Me}) \approx K_D(\text{Ni,ME})/K_D(\text{Me,ME}) \quad (\text{Me,ME} = \text{Mg, Mn, Fe, Co, Zn etc.})$$

Table 6. $K_D(\text{Ni}, \text{Me})$ values, with standard deviations when known, for five structure types. Definition: $K_D(\text{Ni}, \text{Me}) = [X_{\text{Ni}}(\text{M}1) \cdot X_{\text{Me}}(\text{M}2)] / [X_{\text{Ni}}(\text{M}2) \cdot X_{\text{Me}}(\text{M}1)]$. The equilibrium temperatures are usually around 1200 K. Values that have been *estimated* as described in the text are given within brackets

Structure type	Sarcopside	Olivine	Orthopyroxene	Tetrametaphosphate	Cabrerite
Reference structure	$\text{Ni}_3(\text{PO}_4)_2$	Ni_2SiO_4	$\text{Mg}_{0.78}\text{Co}_{0.22}\text{SiO}_3$	$\text{Ni}_2\text{P}_4\text{O}_{12}$	$(\text{Ni}, \text{Mg})_3(\text{AsO}_4)_2 \cdot 8\text{H}_2\text{O}$
Reference	(a)	(b)	(c)	(d)	(e)
Space group	$P2_1/a$	$Pbnm$	$Pbca$	$C2/c$	$C2/m$
Point symmetries					
M 1	$\bar{1}$	$\bar{1}$	1	$\bar{1}$	$2/m$
M 2	1	m	1	2	2
Distances					
M 1—O range	2.07—2.10	2.06—2.11	2.02—2.17	1.97—2.15	2.03—2.11
M 1—O average	2.081	2.078	2.080	2.06	2.086
M 2—O range	2.00—2.19	2.04—2.17	1.98—2.47	2.00—2.15	2.06—2.09
M 2—O average	2.084	2.100	2.158	2.07	2.074
Non-linear angles					
O—M 1—O	71.8—96.7°	75.6—104.4°	81.2—97.0°	80.2—99.8°	88.6—97.5°
O—M 2—O	69.1—172.0	73.2—108.0°	69.9—109.9°	80.6—173.6°	85.1—93.1°
K_D values					
$K_D(\text{Ni}, \text{Mg})$	4.0 ± 0.2^f	9.9 ± 0.4^i	1.3^k	10 ± 4^m	18^e
$K_D(\text{Ni}, \text{Co})$	$2.0 \pm 0.1^*$	[2]	[4]	3.2 ± 0.3^m	—
$K_D(\text{Ni}, \text{Zn})$	$4 \pm 1^*$	—	[4]	5.4 ± 1.3^m	—
$K_D(\text{Ni}, \text{Fe})$	$\sim 100^h$	$\sim 10^j$	[8]	—	—
$K_D(\text{Ni}, \text{Mn})$	$6 \pm 1^*$	[50]	[8]	—	—

* This work, * Calvo and Faggiani, 1975, ^b Lager and Meagher, 1978, ^c Hawthorne and Ito, 1978, ^d Nord, 1983a, ^e Giuseppetti and Tadini, 1982, ^f Nord and Stefanidis, 1983, ^g Nord, 1982, ^h Ericsson and Nord, 1984, ⁱ Bish, 1981, ^j Annersten et al., 1982, ^k Ghose et al., 1975, ^m Nord, 1983b

An example will be given. Ghose and Wan (1974) obtained $K_D(\text{Co}, \text{Mg}) = 4.2$ for an olivine hydrothermally prepared at 1420 K. Disregarding the differences in temperature and pressure, $K_D(\text{Ni}, \text{Co})$ may be estimated from $K_D(\text{Ni}, \text{Co}) \approx K_D(\text{Ni}, \text{Mg})/K_D(\text{Co}, \text{Mg}) = 9.9/4.2 \approx 2$ ($Me = \text{Co}$, $ME = \text{Mg}$).

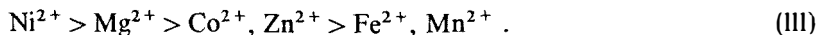
Ghose and Weidner (1974) have reported $K_D(\text{Mn}, \text{Mg}) = 0.196$ for a synthetic Mg-containing tephroite heat-treated at 1270 K. Accordingly, $K_D(\text{Ni}, \text{Mn})$ may be estimated as $9.9/0.196 \approx 50$, so Mn^{2+} would be strongly ordered at M 2 in a (hypothetical) Ni, Mn-olivine. Zinc has not been studied much as a constituent of olivine. The $K_D(\text{Ni}, Me)$ values cited in Table 6 imply the following M 1 site preference order in olivine:



This resembles sequence (I) for the sarcopside structure, although the ordering between iron and manganese has been reversed. The fact that Mg^{2+} and Fe^{2+} are indistinguishable in (II) was expected since it is well established that the distribution is almost random in Mg, Fe-olivines (e.g. Brown, 1980; Nover and Will, 1981). It should finally be mentioned that also in the olivine structure the cation distributions are well correlated to the observed changes in the averaged metal-oxygen distances (cf. Wenk and Raymond, 1973; Bish, 1981).

Survey of $\text{Ni}^{2+}/\text{Me}^{2+}$ cation distributions

Results obtained for orthopyroxenes and some other oxosalt structures will be briefly summarized before a comparison of $\text{Ni}^{2+}/\text{Me}^{2+}$ distributions among octahedral sites resembling those in olivine will be made. Orthopyroxene (*Pbca*) contains two distinct MO_6 octahedra, both without a symmetry element; (M 2) O_6 is larger and more distorted than (M 1) O_6 . From results of Morimoto et al. (1975), Ghose et al. (1975), and Hawthorne and Ito (1978), five $K_D(\text{Ni}, Me)$ values have been derived as exemplified for Ni, Co-olivine (see Table 6). Although the synthesis conditions are not known for all orthopyroxenes involved, the following *approximate* M 1 site preference sequence is indicated:



$\text{Ni}_2\text{P}_4\text{O}_{12}$ (*C2/c*) contains two MO_6 octahedra with $\bar{1}$ and 2 point symmetries; (M 2) O_6 is again slightly larger and somewhat more distorted than (M 1) O_6 (Nord, 1983a). Cation distribution studies of three isostructural $\text{NiMeP}_4\text{O}_{12}$ solid solutions (Nord, 1983b) gave the following M 1 site preference order (cf. Table 6):



Finally, refinement results on the structure of a *cabrerite*, $(\text{Ni},\text{Mg})_3(\text{AsO}_4)_2 \cdot 8\text{H}_2\text{O}$, are included in Table 6. (Cabrerite is a variety of *annabergite*, which has the *vivianite* structure.)

The $K_D(\text{Ni},\text{Me})$ values have been summarized in Table 6, which also includes some crystallographic data for the five structure types. The K_D values clearly show that Ni^{2+} has the greater tendency for the slightly smaller, and somewhat more regular, octahedral "M1" sites, which fact agrees with theoretical considerations (Burns, 1970). As regards the other cations, the results indicate that the size effects are very slight. For instance, the MO_6 octahedra in $\text{Ni}_3(\text{PO}_4)_2$ are almost similar in size, yet the $\text{Ni}^{2+}/\text{Fe}^{2+}$ ordering is stronger in sarcopside than in olivine, where $(\text{M}2)\text{O}_6$ is significantly larger than $(\text{M}1)\text{O}_6$ (cf. Table 6). Furthermore, the $\text{Ni}^{2+}/\text{Mg}^{2+}$ ordering is strong in cabrerite in spite of almost equally sized octahedra, but rather weak in sarcopside. Obviously the $\text{Ni}^{2+}/\text{Me}^{2+}$ distributions in the structures mentioned are mainly controlled by crystal field stabilization energies (CFSE) rather than by size effects. For Mg,Fe-olivine, this has been pointed out by many authors (cf. Nover and Will, 1981). With this in mind, it is logical that the cation ordering is lower, generally speaking, in the orthopyroxenes than in the other structure types, in which M1 and M2 have different point symmetries. However, the present results also clearly show that a large number of complementary cation distribution studies of inorganic and mineral oxosalt structures containing two distinct MO_6 octahedra must be undertaken before any simple empirical relationships governing the distributions, if they exist at all, can be established.

Acknowledgements. I am very grateful to Professor Eric Welin, director of the Mineralogical and Geological departments at the Swedish Museum of Natural History, for his kind interest in my work and for all facilities he has placed at my disposal. I am greatly indebted to my colleague Dr. Bengt Lindqvist for many valuable and inspiring discussions. Many thanks are due to Dr. Arne F. Andresen (Kjeller, Norway) and Mr. Sten Åhlin (Studsvik, Sweden) for their valuable help during the collection of the neutron diffraction data.

This work has received financial support from the Swedish Natural Science Research Council (NFR).

References

- Annersten, H., Ericsson, T., Filippidis, A.: Cation ordering in Ni-Fe olivines. *Am. Mineral.* **67**, 1212-1217 (1982)
- Annersten, H., Nord, A. G.: A high pressure phase of magnesium orthophosphate. *Acta Chem. Scand.* **A34**, 389-390 (1980)
- Berthet, G., Joubert, J. C., Bertaut, E. F.: Vacancies ordering in new metastable orthophosphates $\text{Co}_3\Box(\text{PO}_4)_2$ and $\text{Mg}_3\Box(\text{P}\bullet_4)_2$ with olivine-related structure. *Z. Kristallogr.* **136**, 98-105 (1972)
- Bish, D. L.: Cation ordering in synthetic and natural Ni-Mg olivine. *Am. Mineral.* **66**, 770-776 (1981)
- Brown, G. E.: Olivines and silicate spinels. In: *Orthosilicates* (Ed. P. H. Ribbe), *Reviews in Mineralogy* **5**, 275-381 (1980)

- Burns, R. G.: *Mineralogical applications of crystal field theory*. Cambridge: University Press (1970)
- Calvo, C., Faggiani, R.: Structure of nickel orthophosphate. *Can. J. Chem.* **53**, 1516–1520 (1975)
- Ericsson, T., Nord, A. G.: Strong cation ordering in olivine-related Ni,Fe-sarcopsides. Submitted in June 1983 for publication in *Am. Mineral.* (1984)
- Ghose, S., Wan, C.: Strong site preference of Co^{2+} in olivine, $\text{Co}_{1.10}\text{Mg}_{0.90}\text{SiO}_4$. *Contrib. Mineral. Petrol.* **47**, 131–140 (1974)
- Ghose, S., Wan, C., Okamura, F. P.: Site preference and crystal chemistry of transition metal ions in pyroxenes and olivines. *Acta Crystallogr.* **A31**, S 76 (1975)
- Ghose, S., Weidner, J. R.: Site preference of transition metal ions in olivine. *Geol. Soc. Amer. Abstracts with Programs* **6**, 751 (1974)
- Giuseppetti, G., Tadini, C.: The crystal structure of cabrerite, $(\text{Ni,Mg})_3(\text{AsO}_4)_2 \cdot 8\text{H}_2\text{O}$, a variety of annabergite. *Bull. Minéral.* **105**, 333–337 (1982)
- Hawthorne, F. C., Ito, J.: Refinement of the crystal structures of $(\text{Mg}_{0.776}\text{Co}_{0.224})\text{SiO}_3$ and $(\text{Mg}_{0.925}\text{Mn}_{0.075})\text{SiO}_3$. *Acta Crystallogr.* **B34**, 891–893 (1978)
- Johnson, C. K.: ORTEP – a Fortran thermal-ellipsoid plot program for crystal structure illustrations. ORNL-3794, Oak Ridge, Tenn. (1965)
- Kostiner, E., Rea, J. R.: Crystal structure of ferrous phosphate, $\text{Fe}_3(\text{PO}_4)_2$. *Inorg. Chem.* **13**, 2876–2880 (1974)
- Lager, G. A., Meagher, E. P.: High-temperature structural study of six olivines. *Am. Mineral.* **63**, 365–377 (1978)
- Mattievich, E., Danon, J.: Hydrothermal synthesis and Mössbauer studies of ferrous phosphates of the homologous series $\text{Fe}_3(\text{PO}_4)_2(\text{H}_2\text{O})_n$. *J. Inorg. Nucl. Chem.* **39**, 569–580 (1977)
- Moore, P. B.: Sarcopside: its atomic arrangement. *Am. Mineral.* **57**, 24–35 (1972)
- Morimoto, N., Nakajima, Y., Syono, Y., Akimoto, S., Matsui, Y.: Crystal structures of pyroxene-type ZnSiO_3 and $\text{ZnMgSi}_2\text{O}_6$. *Acta Crystallogr.* **B31**, 1041–1049 (1975)
- Nord, A. G.: A neutron diffraction study of the olivine-related solid solution $(\text{Ni}_{0.75}\text{Zn}_{0.25})_3(\text{PO}_4)_2$. *Neues Jahrb. Mineral.* 422–432 (1982)
- Nord, A. G.: The crystal structure of $\text{Ni}_2\text{P}_4\text{O}_{12}$. *Acta Chem. Scand.* (in press) (1983a)
- Nord, A. G.: Neutron diffraction studies of $\text{NiCoP}_4\text{O}_{12}$ and $\text{NiZnP}_4\text{O}_{12}$. *Mat. Res. Bull.* **18**, 765–773 (1983b)
- Nord, A. G., Ericsson, T.: Cation distributions in $(\text{Fe}_{1-x}\text{Me}_x)_3(\text{PO}_4)_2$ graftonite-type solid solutions determined by Mössbauer spectroscopy. *Z. Kristallogr.* **161**, 209–224 (1982)
- Nord, A. G., Kierkegaard, P.: The crystal structure of $\text{Mg}_3(\text{PO}_4)_2$. *Acta Chem. Scand.* **22**, 1466–1474 (1968)
- Nord, A. G., Stefanidis, T.: Crystal chemistry of γ - $(\text{Zn,Me})_3(\text{PO}_4)_2$ solid solutions. *Mat. Res. Bull.* **16**, 1121–1129 (1981)
- Nord, A. G., Stefanidis, T.: Crystallographic studies of some olivine-related $(\text{Ni,Mg})_3(\text{PO}_4)_2$ solid solutions. *Phys. Chem. Minerals* **10**, 10–15 (1983)
- Nover, G., Will, G.: Structure refinements of seven natural olivine crystals and the influence of the oxygen partial pressure on the cation distribution. *Z. Kristallogr.* **155**, 27–45 (1981)
- Rietveld, H. M.: A profile refinement method for nuclear and magnetic structures. *J. Appl. Crystallogr.* **2**, 65–71 (1969)
- Shannon, R. D., Prewitt, C. T.: Effective ionic radii in oxides and fluorides. *Acta Crystallogr.* **B25**, 925–946 (1969)
- Websky, M.: Sarkopsid, ein neues Mineral aus Schlesien. *Neues Jahrb. Mineral.* 606–607 (1868)
- Wenk, H. R., Raymond, K. N.: Four new structure refinements of olivine. *Z. Kristallogr.* **137**, 86–105 (1973)